

Structure and reactivity of dimeric rhodium(I) formate complexes: X-ray crystal structure analysis of $[(\text{cod})\text{Rh}(\mu\text{-}\kappa^2\text{O},\text{O}'\text{-HCO}_2)]_2$ and phosphane-induced hydride transfer to give an η^3 -cyclooctenyl complex

Roland Fornika, Eckhard Dinjus, Helmar Görls, Walter Leitner^{*,1}

Max-Planck-Gesellschaft zur Förderung der Wissenschaften, Arbeitsgruppe "CO₂ Chemie" an der Universität Jena, Lessingstraße 12, 07743 Jena, Germany

Received 20 July 1995; in revised form 15 September 1995

Abstract

The X-ray crystal structure analysis of $[(L_2)\text{Rh}(\mu\text{-}\kappa^2\text{O},\text{O}'\text{-HCO}_2)_2\text{Rh}(L'_2)]$ **1a** ($L_2 = L'_2 = \text{cod}$) is reported. Complex **1a** reacts with CO to form **1c** ($L = L' = \text{CO}$) via the intermediate **1b** ($L_2 = \text{cod}, L' = \text{CO}$). **1a** and **1c** do not incorporate ¹³CO₂ or D₂ in the formate moiety and are poor catalysts for CO₂ hydrogenation to formic acid. Reaction of **1a** with the chelating phosphanes R₂P(CH₂)₂PR₂ (R = Ph, ⁱPr, Cy) **3a–c** leads to replacement of the diolefin ligand and cleavage of the dimeric structure under formation of monomeric complexes $[(\mathbf{3a-c})_2\text{Rh}][\text{HCO}_2]$ **4a–c**. **4a** was isolated in up to 78% yield and complexes $[(\mathbf{3a})_2\text{RhH}]$ **5a** and $[(\mathbf{3a})\text{Rh}(\eta^3\text{-C}_8\text{H}_{13})]$ **6a** were detected as side products. Complexes of type **6** are formed exclusively under identical reaction conditions using the bidentate ligand Ph₂P(CH₂)₃PPh₂ **3d** or monodentate ligands PAr₃ **3e–f**. A possible mechanism for the formation of complexes **4**, **5** and **6** is discussed involving hydride transfer from the HCO₂[−] ligand to Rh and subsequently to coordinated cod.

Keywords: Carbon dioxide; Rhodium formate complexes; Catalysis; X-ray structure; Hydride transfer; Cyclooctenyl

1. Introduction

The catalytic hydrogenation of CO₂ to formic acid is a field of great current interest, as this reaction provides a promising approach to the use of abundant CO₂ as a chemical feedstock. Although our understanding of the catalytic cycles responsible for CO₂ hydrogenation has greatly improved in recent years, the exact structure of the involved intermediates has still to be elucidated in many cases [1].

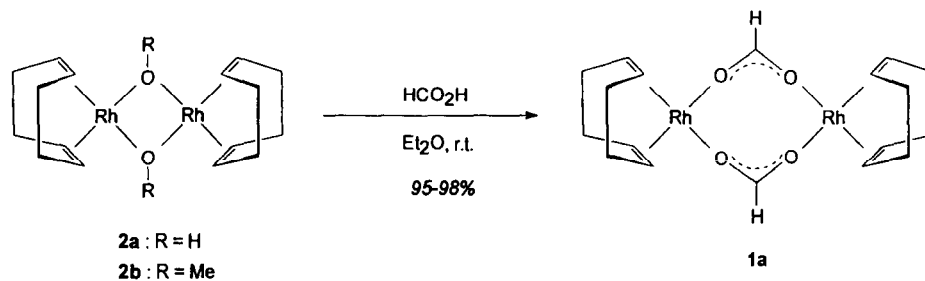
The insertion of CO₂ into the Rh–H bond of 14e species $[(P_2)\text{RhH}]$ (P_2 = chelating bidentate phosphane) to yield formate complexes $[(P_2)\text{Rh}(\text{O}_2\text{CH})]$ has been identified as a key step in rhodium catalysed hydrogenation of carbon dioxide to formic acid in dipolar aprotic solvents [2b,3,4]. Alternatively, it has been suggested

[3] that the insertion could also take place at oligomeric clusters $[(P_2)\text{Rh}(\mu\text{-H})_x]$ [5,6] ($x = 2\text{--}4$). The reversible insertion of CO₂ into a Rh–H bridge has been observed with the A-frame complex $[\text{Rh}_2(\text{CO})_2(\mu\text{-Ph}_2\text{PCH}_2\text{PPh}_2)_2(\mu\text{-H})]^+$ [7], and formate-bridged complexes of iron, tungsten and rhenium have been discussed in the context of CO₂ reduction beyond the formate level [8]. A corresponding catalytic cycle for CO₂ hydrogenation is expected to involve formate-bridged rhodium complexes $[(P_2)\text{Rh}(\mu\text{-HCO}_2)]_n$ as possible intermediates. Only two complexes $[(L_2)\text{Rh}(\mu\text{-HCO}_2)_2\text{Rh}(L'_2)]$ **1a** [9a] ($L_2 = L'_2 = \text{cod}$) and **1c** [9b] ($L = L' = \text{CO}$) have been described in the literature up to now and structural data of rhodium formate complexes are not available [10].

We now report on results of a single crystal X-ray analysis of **1a** and on the reactivity and catalytic behaviour of **1a** and **1c**. In an attempt to synthesize complexes $[(P_2)\text{Rh}(\mu\text{-HCO}_2)]_2$ by reaction of **1a** with monodentate and bidentate phosphanes, we observed a phosphane induced hydride transfer from formate to the

^{*} Corresponding author.

¹ Present address: Max-Planck-Institut für Kohlenforschung, Kaiser-Wilhelm-Platz 1, D-45470 Mülheim/Ruhr, Germany.



Scheme 1.

cyclooctadiene ligand of **1a** that opens a new approach to rhodium η^3 -cyclooctenyl complexes and provides a possible, hitherto neglected, explanation for some special features of rhodium catalysts containing cod as a labile ligand.

2. Results

2.1. Structure of formate-bridged rhodium(I) complexes

Complex **1a** has been obtained for the first time by Keim et al. [9a] from the reaction of $[\{(\text{cod})\text{Rh}(\mu\text{-OR})\}_2]$ **2a** (R = H) or **2b** (R = Me) with methylformate in diethyl ether at room temperature. In our hands, both

complexes **2a–b** remained unchanged, even under prolonged heating, when freshly distilled methylformate was used. However, the reaction proceeds quantitatively when **2a** or **2b** is reacted directly with HCO_2H in diethyl ether (Scheme 1).

Well-formed orange crystals of **1a** suitable for X-ray analysis [11] were obtained from saturated toluene solutions at room temperature. Complex **1a** crystallises in a monoclinic system (space group $C2/c$) and the individual molecules possess a C_2 axis of symmetry perpendicular to the Rh–Rh* -axis and the C1–C1* -axis (Fig. 1). The Rh atoms have a nearly ideal square planar coordination sphere and the two coordination planes form a symmetrical 'butterfly' structure enclosing an angle of $\Theta = 60^\circ$ and resulting in a Rh \cdots Rh distance of 3.39

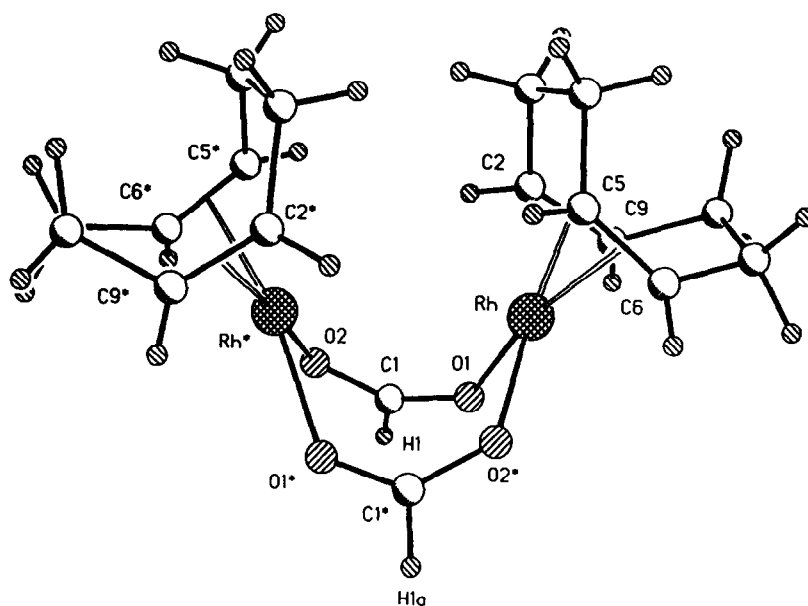
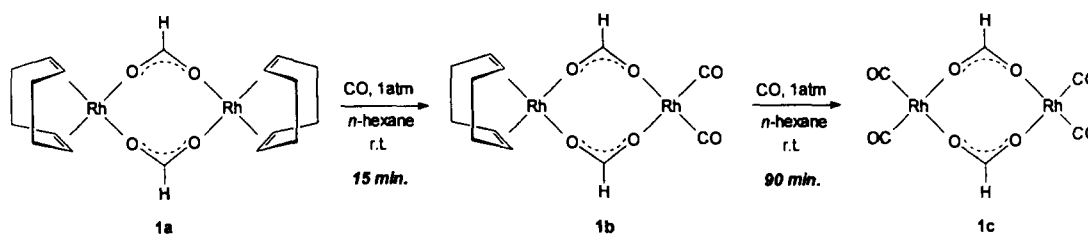


Fig. 1. Molecular structure of $[\{(\text{cod})\text{Rh}(\mu\text{-}\kappa^2\text{O,O}'\text{HCO}_2)\}_2]$ **1a** in the solid state. Selected bond distances (angstroms) and angles (degrees): Rh–O1, 2.101(2); Rh–O2, 2.102(2); Rh–C2, 2.086(2); Rh–C5, 2.105(2); Rh–C6, 2.086(2); Rh–C9, 2.092(3); C2–C9, 1.391(4); C5–C6, 1.396(4); Rh–C2/C9, 1.969(2); Rh–C5/C6, 1.976(2); O1–C1, 1.237(3); O2–C1, 1.239(3); O1–Rh–O2*, 91.3(1); C2–Rh–C5, 82.0(1); C6–Rh–C9, 82.7(1); Rh–O1–C1, 131.7(2); Rh*–O2–C1, 128.4(2); O1–C1–O2, 128.5(2); O1–C1–H1, 116.2(2); O2–C1–H1, 116.2(2).

Table 1
Characteristic spectroscopic data for the formate moiety of complexes $[(L_2)Rh(\mu-\kappa^2O,O'-HCO_2)_2Rh(L'_2)]$ **1a–c**

Complex	IR ^a	¹ H-NMR ^b	¹³ C-NMR ^b
1a (L ₂ =cod, L' ₂ =cod)	$\nu_{as} = 1590\text{ cm}^{-1}$ $\nu_{sym} = 1358\text{ cm}^{-1}$ $\Delta = 232\text{ cm}^{-1}$	$\delta = 7.94\text{ ppm}$ $^3J_{RhH} \leq 3\text{ Hz}$	$\delta = 172.6\text{ ppm}$ $^1J_{CH} = 207\text{ Hz}$
1b (L ₂ =cod, L' ₂ =CO)	$\nu_{as} = 1590\text{ cm}^{-1}$ $\nu_{sym} = 1354\text{ cm}^{-1}$ $\Delta = 236\text{ cm}^{-1}$	$\delta = 7.72\text{ ppm}$ $^3J_{RhH} = 3\text{ Hz}$	$\delta = 172.9\text{ ppm}$ $^1J_{CH} = 211\text{ Hz}$
1c (L=CO, L'=CO)	$\nu_{as} = 1570\text{ cm}^{-1}$ $\nu_{sym} = 1345\text{ cm}^{-1}$ $\Delta = 225\text{ cm}^{-1}$	$\delta = 7.52\text{ ppm}$ $^3J_{RhH} = 3\text{ Hz}$	$\delta = 173.6\text{ ppm}$ $^1J_{CH} = 216\text{ Hz}$

^a As KBr pellets; $\Delta = \nu_{as} - \nu_{sym}$ [14]. ^b In C₆D₆.



Scheme 2.

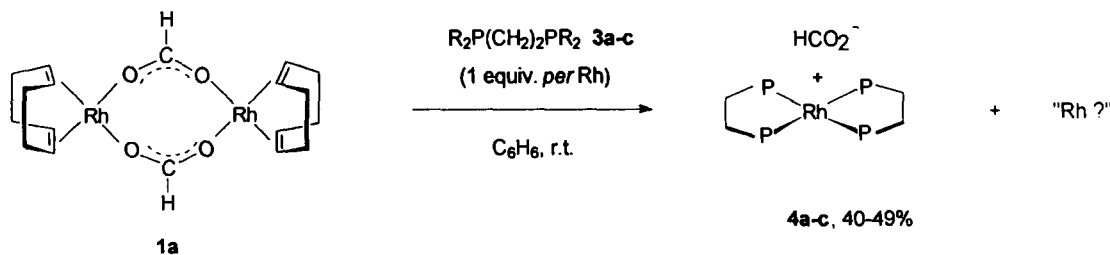
Å. The molecular structure of complex **1a** reveals that the bridging formate moiety adopts a $\mu-\kappa^2O,O'$ coordination mode, as expected from its spectroscopic properties (Table 1). The Rh–O distances and the O–C–O angle are comparable with those found in related bridging carboxylate complexes containing Rh(I) centres [15a,d]. The cod-ligands exhibit their typical slightly twisted boat conformation and the distance of rhodium to the midpoint of the coordinated double bond is with a mean value of 1.97 Å in the characteristic range for dimeric Rh(I)–cod complexes [15a–c].

2.2. Reaction of $[(cod)Rh(\mu-\kappa^2O,O'-HCO_2)]_2$ **1a** with carbon monoxide

Complex **1a** is quantitatively converted to **1c** [9] if a vivid stream of CO is bubbled through a suspension of **1a** in *n*-hexane. If a gentle stream of CO is applied for

only 5 min, deep-red crystals of the hitherto unknown complex **1b** can be isolated (Scheme 2). Only one cod-ligand per dimeric unit is replaced with CO in **1b**, which is an intermediate of the transformation of **1a** to **1c** as shown by further exposure to CO. The stepwise transformation of **1a** to **1b** and subsequently **1c**, together with the almost identical spectroscopic data of the formate bridge in **1a–c** (Table 1), clearly demonstrate that a $\mu-\kappa^2O,O'$ -binding mode is adopted in all three compounds.

The spectroscopic data characteristic for the formate moiety of **1a–c** are summarised in Table 1. The difference Δ between the frequency of the IR active asymmetric (ν_{as}) and symmetric (ν_s) C–O stretching mode of **1a–c** (Table 1) is in the typical range expected for dimeric complexes with a $\mu-\kappa^2O,O'$ -bound formate group [14,16]. The NMR spectroscopic data indicate that this coordination mode is also prevalent in benzene



Scheme 3.

solution and no indication for dissociation into monomeric units is found [9b].

The resonance of the formyl proton of **1a** appears at $\delta = 7.94$ as a slightly broadened singlet owing to coupling with the ^{103}Rh nucleus. The coupling was resolved in the spectra of **1b–c** and $^3J_{\text{RhH}}$ was found to be 3 Hz. Upon subsequent replacement of the cod ligands by CO molecules, a high field shift of $\Delta\delta = 0.2$ is observed in the proton resonance of the formyl group and the coupling constant $^1J_{\text{CH}}$ increases by about 4 Hz. The chemical shift of the sp^2 -carbon appears at somewhat higher field than in related formate bridges [8], and differs only slightly within the series of compounds **1a–c**.

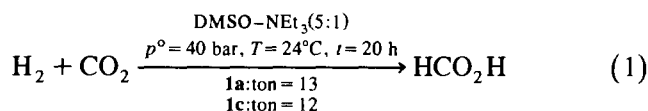
Although complexes **1a–c** are structurally very closely related, they differ considerably in their optical appearance in the solid state and in solution [9]. This can be ascribed at least partly to an increasing $\text{Rh} \cdots \text{Rh}$ interaction in the order **1a** < **1b** < **1c**. A bonding interaction between a filled d_{z^2} and an empty p_z orbital is possible between two square planar Rh(I) fragments, if they are in close proximity and oriented parallel to each other [18]. Steric interactions between the cod ligands in **1a** prevent such an arrangement and lead to the butterfly structure depicted in Fig. 1. Replacement of cod by CO makes a parallel orientation feasible and leads to a shorter $\text{Rh} \cdots \text{Rh}$ distance. Therefore, an effective overlap of orbitals becomes possible and results in a shift of the $\text{M} \rightarrow \text{L}$ charge transfer band to longer wavelengths [18a].

2.3. Catalytic properties of complexes $[(L_2)\text{Rh}(\mu\text{-}\kappa^2\text{O},\text{O}'\text{-HCO}_2)_2\text{Rh}(L'_2)]$ **1a** and **1c**

We have demonstrated recently that the rate of $^{12}\text{CO}_2$ – $^{13}\text{CO}_2$ exchange and of deuterium incorporation into the formate group of rhodium(I) formate complexes $[(\text{P}_2)_2\text{Rh}][\text{HCO}_2]$ correlates qualitatively with the catalytic activity of these compounds in the hydrogenation of carbon dioxide to formic acid [3]. ^1H -NMR spectroscopic studies of **1a** and **1c** under $^{13}\text{CO}_2$ atmosphere showed that neither is able to incorporate labelled car-

bon dioxide. Similarly, no incorporation of D_2 in the formyl position of **1a** or **1c** was observed at ambient pressure. Complex **1a** slowly decomposed under these conditions, while **1c** showed no reactivity at all.

In agreement with this lack of reactivity towards CO_2 and D_2 , both compounds are poor catalysts for the hydrogenation of CO_2 to formic acid under the conditions developed in our group [2]. Only 13 moles of formic acid per mole of rhodium were formed within 20 h in a $\text{DMSO}-\text{NEt}_3$ mixture under a total initial pressure of 40 atm of a 1:1 mixture of CO_2 and H_2 using **1a** as a catalyst ($c(\text{Rh}) = 5 \times 10^{-3} \text{ mol l}^{-1}$). Complex **1c** showed similar low activity leading to the formation of 12 moles of formic acid per rhodium centre.

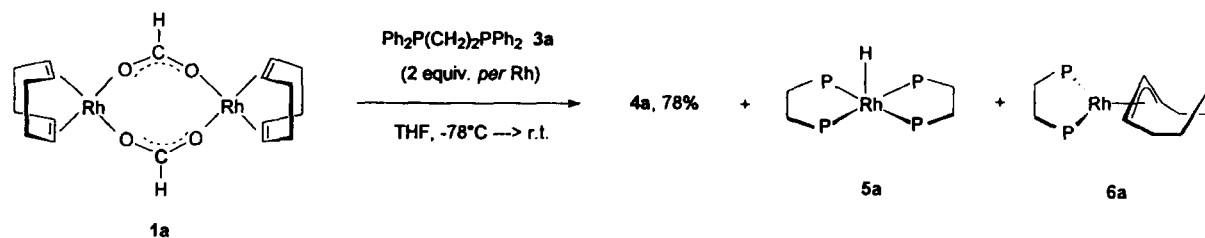


2.4. Reaction of $[(\text{cod})\text{Rh}(\mu\text{-}\kappa^2\text{O},\text{O}'\text{-HCO}_2)_2]$ **1a** with *P*-donor ligands

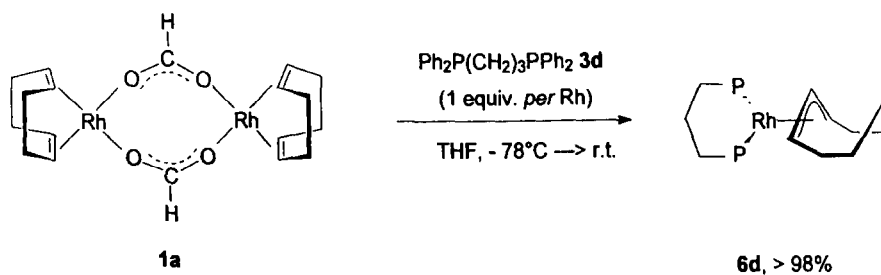
In contrast to the reaction with carbon monoxide, the addition of one equivalent of the chelating phosphane $\text{Ph}_2\text{P}(\text{CH}_2)_2\text{PPh}_2$ **3a** per rhodium centre to a solution of **1a** results in cleavage of the dimeric unit under formation of the monomeric formate complex $[(\text{3a})_2\text{Rh}][\text{HCO}_2]$ **4a** in 45% yield based on rhodium. The same types of product were obtained with other phosphane ligands $\text{R}_2\text{P}(\text{CH}_2)_2\text{PR}_2$ **3b–c** ($\text{R} = ^i\text{Pr}, \text{Cy}$). The fate of the second rhodium centre during these reactions currently remains an open question (Scheme 3).

Similar reaction of **1a** with two equivalents of chelating phosphane **3a** gave **4a** as a major product (78% isolated yield) and by-products $[(\text{3a})_2\text{RhH}]$ **5a** and $[(\text{3a})\text{Rh}(\eta^3\text{-C}_8\text{H}_{13})]$ **6a**. Complexes **5a** and **6a** were formed in an approximate 1:1 ratio, as judged from the ^{31}P -NMR spectrum of the mother liquor immediately after reaction (Scheme 4).

The η^3 -cyclooctenyl complex **6a** was unambiguously characterised by mass spectroscopy and NMR spectro-



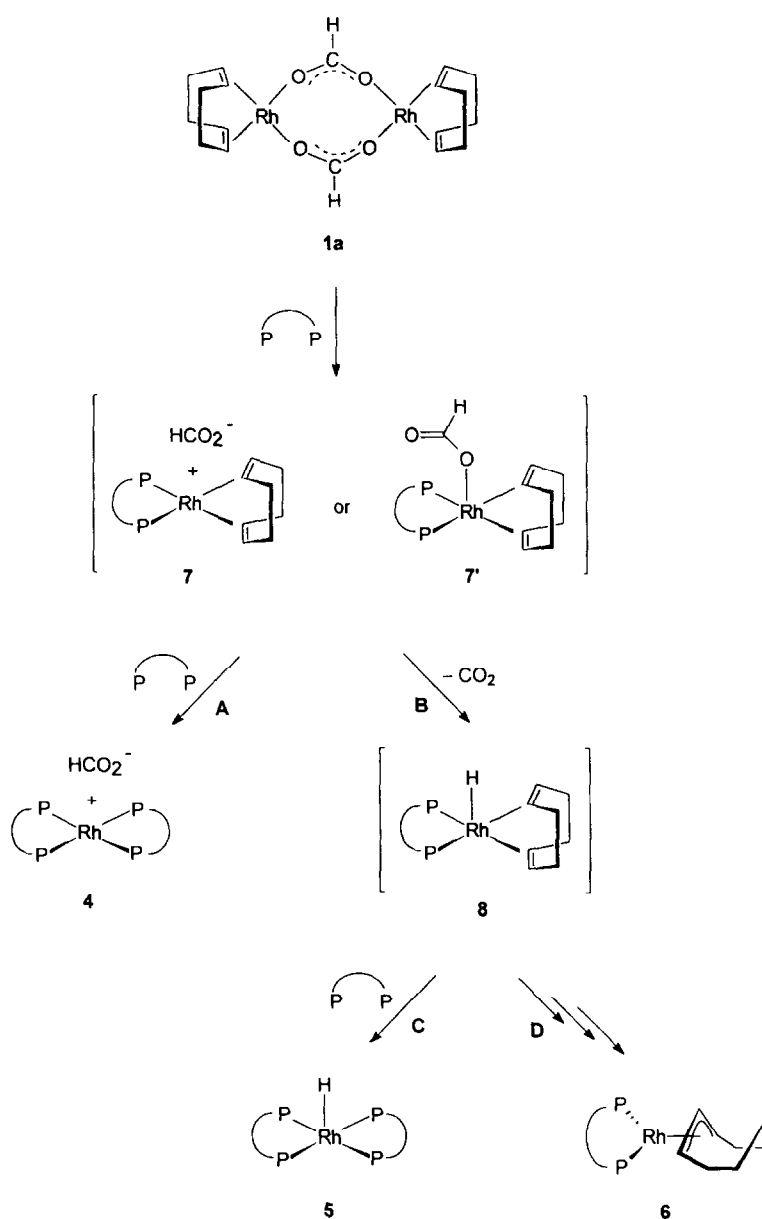
Scheme 4.



Scheme 5.

scopic methods including 1D and 2D homo- and heteronuclear decoupling and correlation experiments. The two chemically equivalent ^{31}P nuclei of the η^3 -cyclooctenyl complex **6a** give rise to a ^{31}P -NMR reso-

nance at $\delta = 68.2$ which appears as a doublet with $^1J_{\text{RhP}} = 199$ Hz. In addition to signals arising from the ligand **3a**, the ^1H -NMR spectrum of **6a** shows a characteristic pattern consisting of a triplet at $\delta = 5.20$ and a

Scheme 6. Mechanistic interpretation of the reaction of $[\{(\text{cod})\text{Rh}(\mu\text{-}\kappa^2\text{O},\text{O}'\text{-HCO}_2)\}_2]$ **1a** with chelating phosphanes.

quartet at $\delta = 4.55$. They integrate in a relative ratio of 1:2 and can be assigned to the protons at position 1 and 2/2' of the η^3 -allyl fragment bound to rhodium [20]

(see Fig. 2 for the numbering scheme). Both sets of signals consist of slightly broadened lines owing to long range coupling with ^{103}Rh and/or ^{31}P . The identical

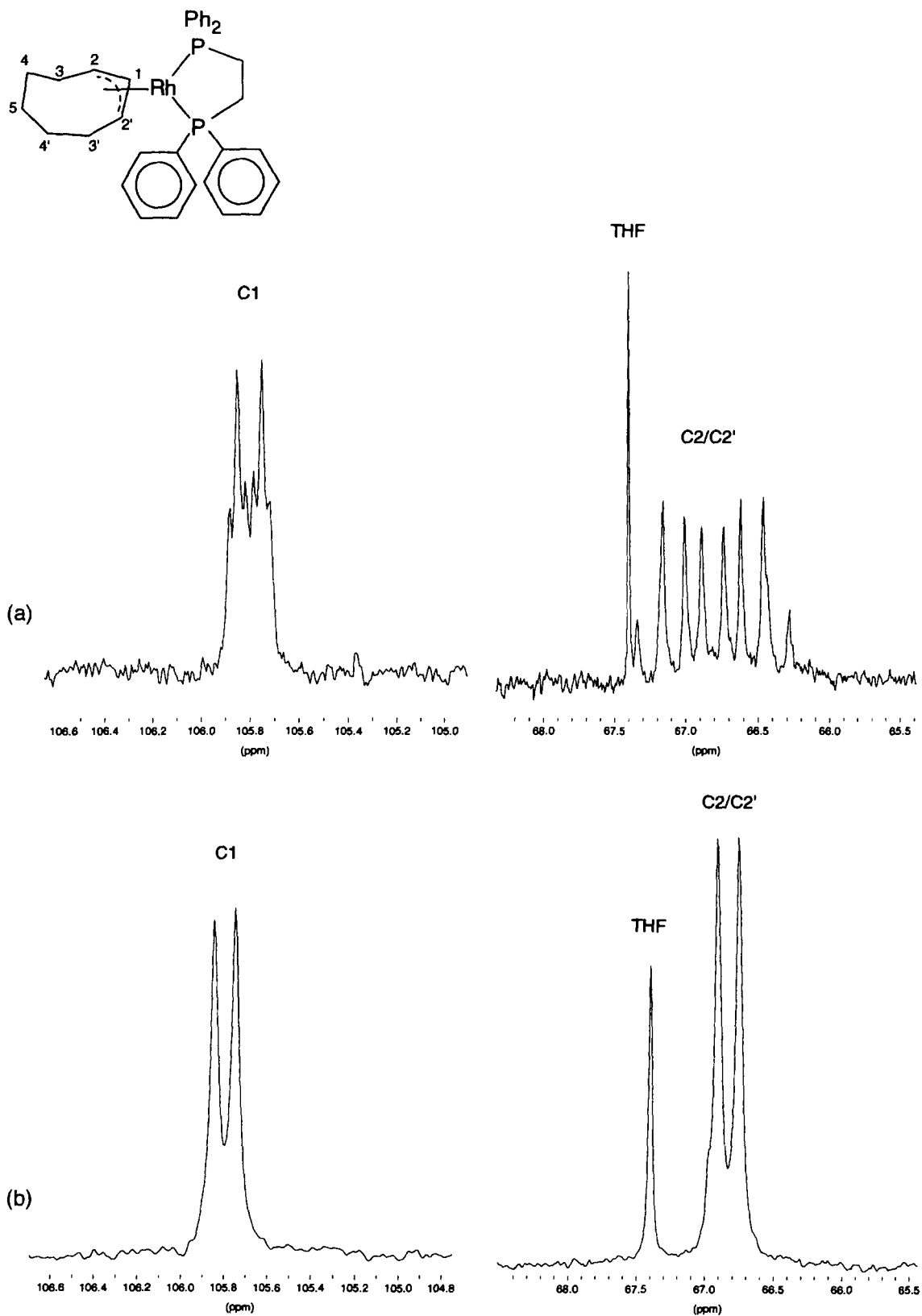


Fig. 2. (a) ¹³C{¹H}-NMR spectrum of 3a in C₆D₆. (b) ¹³C{¹H, ³¹P}-NMR spectrum of 3a in C₆D₆.

coupling constants ${}^3J_{\text{H}_1\text{H}_2} = {}^3J_{\text{H}_1\text{H}_2'} = 7.9$ Hz, together with the small unresolved coupling $J_{\text{H}_2\text{P}}$, are in agreement with a cis-arrangement of the three hydrogen atoms at the η^3 -allyl moiety. The 2D-(${}^1\text{H}$, ${}^1\text{H}$)-COSY spectrum demonstrates that the triplet is only coupled to the quartet, while the latter shares scalar coupling, also with a resonance centred at approximately $\delta = 2.0$. This resonance can, therefore, be assigned to the protons at position 3/3'. The 2D-(${}^{13}\text{C}$, ${}^1\text{H}$)-correlated spectrum shows that the two protons at position 5 exhibit a large difference in chemical shifts $\Delta\delta = 1.0$. This indicates that the cyclooctenyl ligand adopts the expected [21] boat-like structure with the endocyclic proton at position 5 being in close proximity to the η^3 -allyl moiety, resulting in a down field shift of its resonance.

The ${}^{13}\text{C}\{{}^1\text{H}\}$ -NMR spectrum exhibits five carbon resonances in addition to the signals arising from **3a**. The central carbon C1 of the η^3 -allyl moiety appears at $\delta = 105.8$ ppm as a doublet of triplets owing to coupling with ${}^{103}\text{Rh}$ (${}^1J_{\text{RhC}} = 5$ Hz) and two chemically equivalent ${}^{31}\text{P}$ nuclei (${}^2J_{\text{RhP}} = 2$ Hz). The two magnetically inequivalent carbon atoms, C2 and C2', form a higher order spin system giving rise to a signal of eight equally spaced lines centred at $\delta = 66.8$. Both signals collapse to doublets under simultaneous proton and phosphorus decoupling (Fig. 2). Two sets of ${}^{13}\text{C}$ resonances are observed for the individual carbon atoms of the phenyl rings of ligand **3a** in complex **6a**, indicating that possible processes of apparent η^3 -allyl rotation must be considerably slower than the NMR time scale at room temperature.

If complex **1a** is reacted with one equivalent per rhodium of ligand **3d**, forming a six membered rather than a five membered chelate ring, no precipitate is formed and a deep-red solution is obtained initially which turns orange upon warming to room temperature. NMR spectroscopic control of the isolated crude material reveals that the η^3 -cyclooctenyl complex **6d** is formed quantitatively without any by-products, as illustrated in Scheme 5. Complex **6d** exhibits a ${}^{31}\text{P}$ -NMR resonance at $\delta = 27.7$ (${}^1J_{\text{RhP}} = 193$ Hz), other spectroscopic properties being very similar to **6a**.

The cleavage of the dimeric core of **1a** is not restricted to bidentate phosphane ligands. NMR spectroscopic investigations revealed that the use of PPh_3 **3e** leads quantitatively to the cyclooctenyl complex $[(\text{3e})_2\text{Rh}(\eta^3\text{-C}_8\text{H}_{13})]$ **6e** in full analogy to **3d**. The far less basic $\text{P}(p\text{-F-C}_6\text{H}_4)_3$ **3f**, which should resemble the CO ligand even more in its binding properties, also yields **6f** as the sole product.

3. Discussion

Dimeric rhodium(I) formate complexes $[(\text{L}_2)\text{Rh}(\mu\text{-}\kappa^2\text{O},\text{O}'\text{-HCO}_2)_2\text{Rh}(\text{L}'_2)]$ **1a–c** with either cod or CO as

ligands contain bridging formate units that coordinate to the two rhodium centres via both oxygen atoms. These formate bridges are not activated towards ${}^{13}\text{CO}_2$ or D_2 exchange and, consequently, complexes **1a–c** are poor catalysts for CO_2 hydrogenation to formic acid. Earlier results indicate that phosphorus ligands are vital components for rhodium(I) complexes to act as active catalysts in CO_2 hydrogenation [2b]. It is not possible, however, to obtain dimeric formate-bridged complexes of type **1** containing phosphorus donor ligands by cod substitution from **1a**.

The influence of the incoming ligand on the product distribution in the reaction of **1a** with phosphanes is readily explained on basis of the mechanism depicted in Scheme 1. Cleavage of the dimeric core [22] leads to a monomeric rhodium formate complex **7**, which can react with another molecule of **3** to give the bis(phosphane) species **4**. Alternatively, hydride transfer from the formate moiety to rhodium [23b] yields the hydrido complex **8**, which can again be intercepted by phosphane to give **5**. In the case of ligand **3a**, the complex **4a** is known to be stable towards decarboxylation even under much more forcing conditions [3] and can, therefore, be excluded as a possible source for **5a**.

Once the hydrido olefine complex **8** is formed it can undergo insertion of a C=C double bond into the Rh–H bond and subsequent rearrangement of the initially formed π -olefin/ σ -alkyl ligand leads to the thermodynamically stable η^3 -allyl derivative **6**. The ratio of products **4–6** is determined by the relative rates of the four competing pathways A–D in Scheme 1. It is noteworthy in this context that rhodium complexes with phosphane ligands forming six membered chelate rings are much more effective for the activation of the formyl C–H bond of a formate ligand than complexes with five membered rings [3,23].

The present reaction sequence is the first example for the observation of direct hydride transfer from formate to coordinated olefin. A corresponding pathway has been put forward in the mechanism of enantioselective transfer hydrogenation with chiral rhodium phosphane catalysts and formic acid as the hydrogen source [23]. An alternative pathway for the hydride transfer consists of cod substitution in **1a** and subsequent decarboxylation to give $[(\text{P}_2)\text{Rh}(\mu\text{-H})_2]$. Dissociation in $[(\text{P}_2)\text{RhH}]$ and recombination with cod might then lead to **6** [6c,24]. We favour the pathway shown in Scheme 1 in view of the inert character of the formate bridge in **1a** and **1c**.

An intriguing point of the present results is the straightforward and clean formation of the complexes **6d–f** from **1a** and **3d–f** which suggests that η^3 -cyclooctenyl complexes might also be formed under other reaction conditions that produce rhodium monohydrides containing coordinated cod. Such conditions are met when cod complexes are used as catalyst precursors

in hydrogenation reactions under basic conditions [25]. The formation of a relatively stable $[\eta^3\text{-cyclooctenyl}]$ complex thus provides a possible, hitherto neglected, explanation for frequently observed induction periods [2,23,26] and the, in general, lower initial activities observed with catalyst precursors $[(P_2)Rh(cod)]^+$ compared with their norbornadiene analogues [26].

4. Experimental

4.1. General

All reactions involving air- or moisture-sensitive compounds were performed in dry and degassed solvents under argon atmosphere using standard Schlenk techniques. Reaction gases were high purity grade (greater than 4.8) and used without further purification. Formic acid (98%, Merck) was distilled from anhydrous $CuSO_4$, methyl formate (97%, Fluka) was distilled and kept under argon. The organometallic starting materials $[Rh(cod)(OR)]_2$ **2a–b** were prepared as described in the literature [27]. Ligands **3a–b** and **3e–f** were purchased from Strem Chemicals and used as received. **3c–d** were synthesised according to known procedures [28]. Reactions of **1a** and **1c** with D_2 and $^{13}CO_2$ [3] and catalytic runs [2b] were carried out as previously described. NMR measurements were recorded on a Bruker AC 200 spectrometer operating at 200.13, 50.29 and 80.96 MHz for 1H , ^{13}C and ^{31}P . 1H - and ^{13}C -NMR chemical shifts δ are reported in ppm downfield from $SiMe_4$ and referenced to the residual solvent- h_1 and all-deuterated-solvent peaks. ^{31}P -NMR chemical shifts are reported in ppm downfield from phosphoric acid and referenced to external H_3PO_4 . Coupling constants J are reported in Hertz. IR data were recorded on a Perkin Elmer 16 PC FT-IR spectrophotometer, mass spectra on a Finnigan MAT SSQ 710.

4.2. Synthesis of $[{(cod)Rh(\mu-HCO_2)}_2] \mathbf{1a}$

A suspension of **2a** (505 mg, 1.11 mmol) in 13 ml diethyl ether was treated with three drops of formic acid. The colour of the suspension immediately turned

from yellow to a slight orange. The reaction mixture was stirred for 10 min at room temperature and the resulting slight orange crystalline precipitate was filtered off, washed with ether and dried in vacuo to give 545 mg of complex **1a** (1.06 mmol; 96%). The same procedure is applicable to the synthesis of **1a** from **2b** in 98% yield.

4.3. Reaction of $[{(cod)Rh(\mu-HCO_2)}_2] \mathbf{1a}$ with CO

4.3.1. Preparation of $[{(CO)_2Rh(\mu-HCO_2)}_2] \mathbf{1c}$

100 mg (0.20 mmol) of **1a** were suspended in 15 ml of *n*-hexane. For 1.5 h, a strong stream of CO was bubbled through the suspension. The yellow reaction mixture turned into a red-brown colour within a few minutes. Filtration and drying the residue in vacuo gave 69.3 mg (17.0 mmol, 87%) of **1c** as needles of a brass-like colour.

4.3.2. Preparation of $[{(CO)_2Rh(\mu-HCO_2)}_2Rh(cod)] \mathbf{1b}$

150 mg (0.29 mmol) of **1a** were suspended in 15 ml of *n*-hexane. For 5 min, a gentle stream of CO was bubbled through the suspension. After removing the solvent in vacuo, the residue was dried and redissolved in 5 ml benzene. The red solution was filtered off and removal of the solvent gave 38.6 mg (0.08 mmol; 29%) **1b** as dark red small plates.

1H -NMR (C_6D_6) δ : 1.33 (m, br, 4H, $-CH_2$); 2.21 (m, br, 4H, $-CH_2$); 4.06 (m, br, 4H, $=C-H$); 7.72 (t, 2H, O_2C-H , $^3J_{RhH} = 3$) ppm.

$^{13}C\{^1H\}$ -NMR (C_6D_6) δ : 30.6 (s, $-CH_2$); 76.5 (s, br, $=C-H$); 172.9 (s, O_2C-H , gated decoupling: d, $^1J_{CH} = 211$); 183.8 (d, $-C\equiv O$, $^1J_{RhC} = 73$) ppm.

IR (KBr) ν (cm^{-1}): 2946(w), 2874(w), 2838(w), 2100(w), 2078(vs), 2010(vs), 1590(vs), 1372(m), 1354(s), 1326(m).

4.4. Reaction of $[{(cod)Rh(\mu-HCO_2)}_2] \mathbf{1a}$ with $R_2P(CH_2)_2PR_2$ **3a–c**

4.4.1. Reaction of **1a** with one equivalent of **3a–c**

238 mg (0.47 mmol) of **1a** were dissolved in 20 ml of benzene and 0.47 mmol of the appropriate phosphane **3a–c** in 15 ml of benzene were slowly added within 20

Table 2
Characteristic spectroscopic data for complexes **4a–c**

Complex	δ (1H) ^a	δ (^{31}P) ^a	$^1J_{RhP}$ ^a	Δ (cm^{-1}) ^b
4a	8.55 (8.76)	58.8 (58.2)	133 (132)	295
4b	8.55 (8.96)	(66.2)	(128)	310
4c	(8.91)	(72.8)	(128)	250

^a In $DMSO-d_6$; values in parentheses are in $CDCl_3$; complexes **4a–c** are only moderately stable in $CDCl_3$. ^b As KBr pellets.

min at room temperature with a Teflon cannula. After complete addition the reaction mixture was stirred for 20 min. The bright yellow precipitate was filtered off, washed with benzene (5 ml) and pentane (5 ml) and dried in vacuo to give **4a–c** (40–49%). Characteristic spectroscopic data are given in Table 2.

4.4.2. Reaction of **1a** with two equivalents of **3a**; isolation of $[(3a)Rh(\eta^3-C_8H_{13})]$ **6a**

250 mg (0.49 mmol) of **1a** were dissolved in 20 ml of THF and cooled to -78°C in an acetone–dry ice bath. A solution of **3a** (389 mg, 0.98 mmol) in 15 ml of THF was added slowly under continuous stirring within 20 min with a Teflon cannula. The resulting mixture was allowed to warm to room temperature and stirred for 30 min. The solvent was removed, and the residue was redissolved in 5 ml benzene. The resulting yellow precipitate was filtered off, washed with pentane (5 ml) and dried in vacuo to give 78% of **4a**. The benzene filtrate was evaporated to dryness and the residue was redissolved in cold THF (5 ml), producing an orange precipitate which was filtered off and identified as **5a**. The filtrate was again evaporated to give an ochre solid that was analysed by NMR and mass spectroscopy. Characteristic NMR data for **6a** are given in Table 3.

M.p. 230°C (dec.) under Ar. MS (EI, 70 eV) m/z : 610 (M^+), 501 ($M^+ - C_8H_{13}$), 424 ($M^+ - C_8H_{13} - C_6H_5$). $^1\text{H-NMR}$ (C_6D_6 , phosphane fragment only): 1.8–2.2 (CH_2-P , 4H, m), 6.8–7.3 (PPh, *o,p*-H, 12H, m), 7.5–8.0 (PPh, *m*-H, 8H, m).

$^{13}\text{C}\{^1\text{H}\}$ -NMR (C_6D_6 , phosphane fragment only): 30.6 (CH_2-P , dt, $|^1J_{PC} + ^3J_{PC}| = 12$, $^2J_{RHC} = 2$); 139.7–140.2 (PPh, *ipso*-C, m); 132.3/132.9 (PPh, *o*-C,

t, $|^2J_{PC} + ^4J_{PC}| = 6$); 127.7/127.9 (PPh, *m*-C, t, $|^3J_{PC} + ^5J_{PC}| = 5$); 128.4/128.6 (PPh, *p*-C, s).

4.4.3. Synthesis of $[(Ph_2P(CH_2)_3PPh_2)Rh(\eta^3-C_8H_{13})]$ **6d**

250 mg (0.49 mmol) of **1a** were dissolved in 20 ml of THF and cooled to -78°C in a acetone–dry ice bath. A solution of **3d** (202 mg, 0.49 mmol) in 15 ml of THF was added slowly under continuous stirring within 20 min with a Teflon cannula. The resulting clear solution was stirred for 30 min at room temperature. The solvent was removed and the yellow residue was dried in vacuo for 1 day to give 300 mg (0.48 mmol; 98%) **6d** containing small amounts of THF according to proton NMR analysis. Characteristic NMR spectroscopic data of **6d** are given in Table 3.

M.p. 230°C (dec.) under Ar. MS (EI, 70 eV) m/z : 624 (M^+), 515 ($M^+ - C_8H_{13}$), 438 ($M^+ - C_8H_{13} - C_6H_5$).

$^1\text{H-NMR}$ (C_6D_6 , phosphane fragment only): 1.5–1.8 (CH_2-CH_2-P , 2H, m), 2.1–2.4 (CH_2-P , 4H, m), 6.7–7.3 (PPh, *o,p*-H, 12H, m), 7.4–7.8 (PPh, *m*-H, 8H, m).

$^{13}\text{C}\{^1\text{H}\}$ -NMR (phosphane fragment only): 30.5 (CH_2-P , dt, $|^1J_{PC} + ^3J_{PC}| = 12$, $^2J_{RHC} = 2$); 20.2 (CH_2-CH_2-P , t, $|^2J_{PC} + ^4J_{PC}| = 4$); 139.4–139.8 (PPh, *ipso*-C, m); 132.4/132.9 (PPh, *o*-C, t, $|^2J_{PC} + ^4J_{PC}| = 7$); 127.4/127.6 (PPh, *m*-C, t, $|^3J_{PC} + ^5J_{PC}| = 4$); 128.0/128.3 (PPh, *p*-C, s).

4.4.4. Reaction of **1a** with monodentate phosphanes PPh_3 **3e** and $P(p-F-C_6H_4)_3$ **3f**

The reactions were performed by reacting **1a** (25.0 mg, 0.05 mmol) in 0.5 ml THF- d_8 with two equivalents

Table 3
Characteristic NMR spectroscopical data for η^3 -cyclooctenyl complexes **6a–f**

Complex	$^{31}\text{P}\{^1\text{H}\}$ -NMR δ (ppm)	^1H -NMR δ (ppm)	$^{13}\text{C}\{^1\text{H}\}$ -NMR δ (ppm)
6a ^a	68.2 (d, $J_{RHP} = 199$)	5.20 (1, t, 1H, $^3J_{HH} = 7.9$); 4.55 (2/2', q, 2H, $^3J_{HH} = 7.9$); 1.8–2.3 (3/3', m, 4H); 1.3–1.8 (4/4', m, 4H); 1.3–1.5 (5 ^{exo} , m 1H), 2.3–2.5 (5 ^{endo} , m, 1H).	105.8 (1, dt, $^1J_{RHC} = 5$, $^2J_{PC} = 2$); 66.8 (2/2', m, $^1J_{RHC} = 8$ ^b); 33.2 (3/3', d, $^3J_{RHC} = 2$); 30.9 (4/4', t, $ ^4J_{PC}(\text{trans}) + ^4J_{PC}(\text{cis}) = 8$ Hz); 23.6 (5, s).
6d ^a	27.7 (d, $J_{RHP} = 193$)	5.23 (1, t, 1H, $^3J_{HH} = 8.0$); 3.80 (2/2', q, 2H, $^3J_{HH} = 8.0$); 1.4–2.0 (3/3', m, 4H); 1.2–1.6 (4/4', m, 4H); 1.1–1.4 (5 ^{exo} , m 1H), 2.1–2.4 (5 ^{endo} , m, 1H).	104.7 (1, dt, $^1J_{RHC} = 5$, $^2J_{PC} = 2$); 68.6 (2/2', m); 32.6 (3/3', d, $^3J_{RHC} = 2$); 30.4 (4/4', t, $ ^4J_{PC}(\text{trans}) + ^4J_{PC}(\text{cis}) = 8$ Hz); 23.4 (5, s).
6e ^c	43.3 (d, $J_{RHP} = 202$)	5.13 (1, t, 1H, $^3J_{HH} = 8.0$); 3.29 (2/2', q, 2H, $^3J_{HH} = 8.0$).	–
6f ^{c,d}	41.3 (d, $J_{RHP} = 204$)	5.24 (1, t, 1H, $^3J_{HH} = 8.2$); 3.55 (2/2', q, 2H, $^3J_{HH} = 8.2$).	–

^a In C_6D_6 ; see Fig. 2 for numbering scheme. ^b From a $^{13}\text{C}\{^1\text{H}, ^{31}\text{P}\}$ experiment. ^c In THF- d_8 . ^d $^{19}\text{F}\{^1\text{H}\}$ -NMR: $\delta = -103.2$.

of **3e–f** directly in an NMR-tube. Characteristic ^1H - and ^{31}P -NMR data for **6e–f** are given in Table 3.

Acknowledgement

Financial support by the Fonds der Chemischen Industrie and the Max-Planck-Gesellschaft is gratefully acknowledged. We wish to thank Degussa AG for a generous loan of $\text{RhCl}_3 \cdot 3\text{H}_2\text{O}$.

References and notes

- [1] (a) P.G. Jessop, T. Ikariya and R. Noyori, *Chem. Rev.*, **95** (1995) 259; (b) W. Leitner, *Angew. Chem.*, **107** (1995) 2391; *Angew. Chem. Int. Ed. Engl.*, **34** (1995) 2207.
- [2] (a) E. Graf and W. Leitner, *J. Chem. Soc. Chem. Commun.*, (1992) 623; (b) W. Leitner, E. Dinjus and F. Gaßner, *J. Organomet. Chem.*, **475** (1994) 257; (c) R. Fornika, H. Görls, B. Seemann and W. Leitner, *J. Chem. Soc. Chem. Commun.*, (1995) 1479.
- [3] T. Burgemeister, F. Kastner and W. Leitner, *Angew. Chem.*, **105** (1993) 781; *Angew. Chem. Int. Ed. Engl.*, **32** (1993) 739.
- [4] F. Hutschka, A. Dedieu and W. Leitner, *Angew. Chem.*, **107** (1995) 1905; *Angew. Chem. Int. Ed. Engl.*, **34** (1995) 1742.
- [5] (a) V.W. Day, M.F. Fredrich, G.S. Reddy, A.J. Sivak, W.R. Pretzer and E.L. Muetterties, *J. Am. Chem. Soc.*, **99** (1977) 8091; (b) A.J. Sivak and E.L. Muetterties, *J. Am. Chem. Soc.*, **101** (1979) 4878; (c) H.K.A.C. Coolen, R.J.M. Nolte and P.W.N.M. van Leeuwen, *J. Organomet. Chem.*, **496** (1995) 159.
- [6] (a) M.D. Fryzuk, *Can. J. Chem.*, **61** (1983) 1347; (b) M.D. Fryzuk, T. Jones and F.W.B. Einstein, *Organometallics*, **3** (1984) 185; (c) M.D. Fryzuk, W.E. Piers, S.J. Rettig, F.W.B. Einstein, T. Jones and T.A. Albright, *J. Am. Chem. Soc.*, **111** (1989) 5709; (d) M.D. Fryzuk, W.E. Piers, F.W.B. Einstein and T. Jones, *Can. J. Chem.*, **67** (1989) 883; (e) M.D. Fryzuk and W.E. Piers, *Organometallics*, **9** (1990) 986.
- [7] C.P. Kubiak, C. Woodcock and R. Eisenberg, *Inorg. Chem.*, **21** (1982) 2119.
- [8] (a) C.C. Tso and A.R. Cutler, *Organometallics*, **4** (1985) 1242; (b) C.C. Tso and A.R. Cutler, *Inorg. Chem.*, **29** (1990) 471.
- [9] (a) W. Keim, J. Becker and A.M. Trzeciak, *J. Organomet. Chem.*, **372** (1989) 447; (b) F. Pruchnik and K. Wajda, *Inorg. Chim. Acta*, **40** (1980) 203.
- [10] (a) For a detailed discussion of the possible coordination modes of the formate ligand see G. Busca and V. Lorenzelli, *Mater. Chem.*, **7** (1982) 89.
(b) Unsuccessful attempts to synthesis complexes. $[(\text{P}_2)\text{Rh}(\mu\text{-HCO}_2)_2]$ via a route similar to the one outlined for **1a** were reported while this paper was in print. They lead to a monomeric Rh(I) formate complex that was shown by X-ray diffraction to contain a κO -bound formate unit: V.V. Grushin, V.F. Kuznetsov, C. Bensimon and H. Alper, *Organometallics*, **14** (1995) 3927.
- [11] X-ray crystal structure determination of **1a**. Data were collected on an Enraf-Nonius CAD4 diffractometer with graphite-monochromated Mo K α radiation. The $\omega/2\theta$ -scan technique was used with variable scan width $\Delta\omega = (0.65 + 0.35\tan\theta)$, a max. scan speed of 10.0 min^{-1} in ω and a max. scan time of 30 s per reflection. The unit cell parameters were determined from a least squares refinement of 25 reflections with $17.7 < \theta < 24.6^\circ$. Data were corrected for Lorentz polarization and absorption effects. The structure was solved by the heavy-atom method using SHELXS-86 [12a] and was subjected to least squares refinement on F with 161 positional and anisotropic thermal parameters for all nonhydrogen atoms using MOLEN [12b]. The H-atoms were calculated by assuming C–H distance of 0.96 \AA and refined with an overall temperature factor. Scattering factors and anomalous-dispersions corrections were taken from *International Tables for X-Ray Crystallography* [13]. Further details of the crystal structure investigation may be obtained from the Fachinformationszentrum Karlsruhe, D-76344 Eggenstein-Leopoldshafen 2, on quoting the depository number CSD-217, names of the authors and the journal citation.
Crystal data for 1a. Empirical formula: $\text{C}_{18}\text{H}_{26}\text{O}_4\text{Rh}$; colour: orange; formula weight: $512.22 \text{ g mol}^{-1}$; crystal system: monoclinic; crystal size: $0.51 \times 0.24 \times 0.08 \text{ mm}^3$; space group: $C2/c$ (No. 15); cell constants: $a = 12.866(3)$, $b = 11.746(2)$, $c = 11.840(1) \text{ \AA}$; volume: $1772.2(6) \text{ \AA}^3$; temperature: $T 20(1)^\circ\text{C}$; density (calc): $D_c = 1.92 \text{ g cm}^{-3}$; molecules per unit cell: $Z = 4$; absorption coefficient: 18.5 cm^{-1} ; absorption correction: psi-scan; $T_{\text{min}}/T_{\text{max}}$: $0.965/1.000$; $\sin\theta_{\text{max}}/\lambda = 0.677$; radiation: Mo K α ($\lambda = 0.71069 \text{ \AA}$); total no. of reflections: 3320; no. of independent reflections: 3059; no. of observed reflections ($I > 2\sigma(I)$): 2585; final R indices: $R = 0.025$, $R_w = 0.035$; no. of parameters refined: 161; goodness of fit: 1.35; residual electron density: 0.43 e \AA^{-3} .
- [12] (a) G.M. Sheldrick, SHELXS-86, A computer program for crystal structure determination, University of Göttingen, Germany, 1986; (b) MOLEN, An interactive structure solution procedure, Enraf-Nonius, Delft, Netherlands, 1990.
- [13] *International Tables for X-Ray Crystallography*, Vol. 4, Kynoch, Birmingham, UK, 1974.
- [14] (a) D.B. Deacon and R.J. Phillips, *Coord. Chem. Rev.*, **33** (1980) 227; (b) K. Nakamoto, *Infrared and Raman Spectra of Inorganic and Coordination Compounds*, Wiley, New York, 1986, 4th edn.
- [15] (a) W.S. Sheldrick and B. Günther, *J. Organomet. Chem.*, **375** (1989) 233; (b) J.A. Ibers and R.G. Snyder, *Acta Crystallogr.*, **15** (1962) 923; (c) L.F. Dahl, C. Martell and D.L. Wampler, *J. Am. Chem. Soc.*, **83** (1961) 1761; (d) G. Meister, G. Rheinwald, H. Stoeckli-Evans and G. Süss-Fink, *J. Organomet. Chem.*, **496** (1995) 197.
- [16] A survey of unambiguously characterised formate complexes published up to the present date leads to the following ranges for typical Δ values: $\kappa^2\text{O,O'}$: 190 to 225 cm^{-1} , similar to ionic formates ($\text{Na}[\text{HCO}_2]$: $\Delta = 235 \text{ cm}^{-1}$ [17a]); κO : 290 to 380 cm^{-1} ; $\mu\text{-}\kappa^2\text{O,O'}$: 210 to 250 cm^{-1} . The bridging of two metals by only one oxygen atom of a formate ligand ($\mu\text{-}\kappa\text{O}$) has been demonstrated by X-ray diffraction [17b,c], but the assignment of the IR frequencies is not conclusive as this binding mode was always accompanied by $\mu\text{-}\kappa^2\text{O,O'}$ formate bridges. Nevertheless, Δ values greater than 300 cm^{-1} can be predicted for a $\mu\text{-}\kappa\text{O}$ -bound formate by extrapolation of the data from Ref. [14].
- [17] (a) W.H. Zachariasen, *J. Am. Chem. Soc.*, **62** (1940) 1011; (b) W.B. Tolman, A. Bino and S.J. Lippard, *J. Am. Chem. Soc.*, **111** (1989) 8522; (c) W.B. Tolman, S. Liu, J.G. Bentsen and S.J. Lippard, *J. Am. Chem. Soc.*, **113** (1991) 152.
- [18] (a) A.L. Bulch and B. Talyathan, *Inorg. Chem.*, **16** (1977) 2840; (b) J.J. Novoa, G. Aullon, P. Alemany and S. Alvarez, *J. Am. Chem. Soc.*, **117** (1995) 7169.
- [19] (a) A. Sacco and R. Ugo, *J. Chem. Soc.*, (1964) 3274; (b) B.R. James and D. Mahajan, *Can. J. Chem.*, **57** (1979) 180.
- [20] (a) M.D. Fryzuk, *Inorg. Chem.*, **21** (1982) 2134; (b) R. Wiedemann, J. Wolf and H. Werner, *Angew. Chem.*, **107** (1995) 1359.

- [21] K. Jonas, *Angew. Chem.*, 97 (1985) 292.
- [22] (a) A.R. Sanger, *J. Chem. Soc. Dalton Trans.*, (1977) 120; (b) R.R. Schrock and J.A. Osborn, *J. Am. Chem. Soc.*, 93 (1971) 2397; (c) B.R. James, R.H. Morris and K.J. Reimer, *Can. J. Chem.*, 55 (1977) 2352; (d) a similar cleavage was recently observed using chelating P \cap O ligands: E. Lindner, Q. Wang, H.A. Mayer and A. Bader, *J. Organomet. Chem.*, 458 (1993) 229.
- [23] (a) H. Brunner and W. Leitner, *Angew. Chem.*, 100 (1988) 1231; *Angew. Chem. Int. Ed. Engl.*, 27 (1988) 1180; (b) W. Leitner, J.M. Brown and H. Brunner, *J. Am. Chem. Soc.*, 115 (1993) 152.
- [24] (a) C.A. Reilly and H. Thyret, *J. Am. Chem. Soc.*, 89 (1967) 5144; (b) A.W. Cordes, S. Siegel, S.-T. Lin, L. Martin and M.C. Noble, *Acta Crystallogr. Sect. C*, 46 (1990) 494.
- [25] (a) R.R. Schrock and J.A. Osborn, *J. Am. Chem. Soc.*, 98 (1976) 2134; (b) P.A. Chaloner, M.A. Esteruelas, F. Joó and L.A. Oro, *Homogeneous Hydrogenation*, Kluwer, Dordrecht, 1994, p. 21.
- [26] D. Heller, K. Kortus and R. Selke, *Liebigs Ann.*, (1995) 575.
- [27] R. Uson, L.A. Oro and J.A. Cabeza, *Inorg. Synth.*, 23 (1983) 126.
- [28] R.J. Burt, J. Chatt, W. Hussain and G.J. Leigh, *J. Organomet. Chem.*, 182 (1979) 203.